Magnesium Technology 2011
Edited by: Wim H. Sillekens, Sean R. Agnew, Neale R. Neelameggham, and Suveen N. Mathaudhu
TMS (The Minerals, Metals & Materials Society), 2011

PROCESSING ASPECTS OF MAGNESIUM ALLOY STENT TUBE

R.J. Werkhoven, W.H. Sillekens, J.B.J.M. van Lieshout
TNO Science and Industry; PO Box 6235; 5600 HE Eindhoven, Netherlands

Keywords: Biomedical Implants, Stents, Equal Channel Angular Pressing, Extrusion, Drawing

Abstract

Biomedical applications are an emerging field of interest for magnesium technology, envisioning biodegradable implants that resorb in the human body after having cured a particular medical condition (such as artery clogging or bone fractures). This challenges research in a sense that the materials to be used need to dissolve *in vivo* in a controlled fashion without leaving harmful remainders and while maintaining sufficient strength and other (mechanical) attributes as long as necessary.

To comply to the requirements, magnesium alloys as well as their processing routes into implants need to be tailored. While new alloy compositions are receiving ample attention, the paper at hand addresses the processing issue. The application of choice is the (cardio)-vascular stent. Different steps in manufacturing magnesium AZ-alloy stent tube are considered, including equal channel angular pressing, extrusion and subsequent drawing operations. Results show that the processing route has an important influence on the microstructure of the finished stent tube and hence on its functional performance.

Introduction

Life expectancy has increased considerably over the last fifty years due to the many advances in healthcare. In line with this, the market for implantable medical devices is booming due to upward trends in medical conditions and patient activity, changing patient treatment approaches and technical advances. For instance, the demand for cardiac implants quadrupled, for orthopaedic implants doubled and for all other implants tripled between 1997 and 2007 [1].

Current (metallic) biomaterials for these implants are essentially neutral *in vivo*. Such bio-passive implants remain either in the body (with the risk of loosening, fracturing and tissue inflammation) or are explanted after healing (implying additional surgical risk, patient discomfort and costs). Degradable materials that are under development – notably polymers – partially meet these drawbacks as they do need less repeated invasive surgery, since once absorbed they leave behind only the healed natural tissue. Further trends are towards surface modification of biomaterials to better control blood and tissue compatibility, implants and devices that are also vehicles for drug delivery, and the development of new classes of biomaterials for tissue engineering.

As for magnesium, its biocompatibility including its *in vivo* resorption (corrosion in the electrolytic environment of the body), supposed non-toxicity to the human body, as well as its functional role in the physiological system render it an interesting candidate for degradable implants. Its mechanical properties – notably strength and modulus of elasticity – as well as its density are quite similar to natural bone material and hence of interest for hard-tissue engineering applications.

Pioneering work in the mid-20th century indicated a significant reduction in healing time and acceleration in mineralization of bone fractures, while no toxic effects were observed [2]. The formation of hydrogen in the corrosion process, however, posed a problem and the interest shifted in favor of stainless steel and titanium. It was not before the late 1970's that corrosion resistance was substantially improved by the use of specific alloying elements and high-purity alloys, so that hydrogen formation was suppressed as well and implanted styles remained *in vivo* for months. Most recently the use of magnesium for medical applications has seen a growing research interest, also because of its perceived osteo-conductive activity (favoring bone apposition). The current state-of-the-art for biomedical implants and the envisaged role for magnesium are outlined in **Figure 1**.

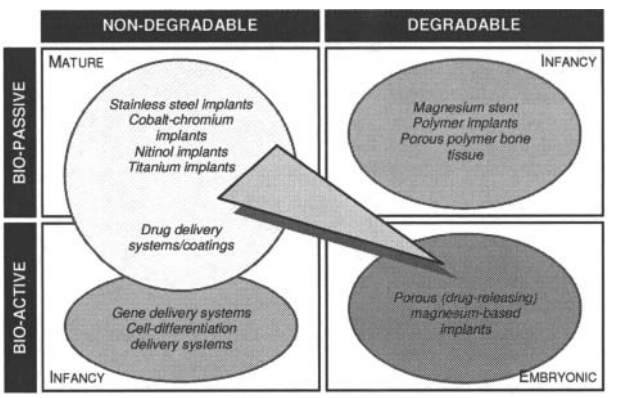

Figure 1. Trends in biomedical implants (represented by the arrow) and the position of magnesium.

As one of the targeted applications, the development of magnesium (cardio)-vascular stents is currently being undertaken with initial successes reported [3–5]. Stents are implants that are surgically placed in clogged arteries to restore adequate blood flow. A stent essentially consists of a thin-walled mesh tube with typical overall dimensions being 3 mm in diameter and 20 mm in length. Wall thickness and strut size can be as low as 100–150 µm. A stent is implanted by shrinking it on a balloon catheter and subsequently expanding it upon proper positioning in the artery. Thus, the stent material must comply to such mechanical requirements as strength and ductility in addition to biological demands, as indicated in **Table I**. Apart from these, there are supplementary requirements for stents that are not listed but also relevant, such as on geometrical accuracy, manufacturability and fatigue resistance.

While in the early investigations the commercial-grade alloy WE43 was used, more recently a variety of other alloy systems has been proposed. This also includes alloy modifications with calcium, aluminum or lithium as the primary alloying element [6–9]. Main objective of these efforts is to slow down resorption (or

corrosion) rate while maintaining or improving mechanical properties. Although not all biocompatibility effects of the alloying elements are cleared and certification remains a concern, magnesium alloy stents (with an indicative weight of 5 mg) are among the least mass-critical as compared to other implants.

Table I. Primary requirements for magnesium alloy stent tube.

ASPECT	DESCRIPTION
Resorption	Scaffolding integrity 3–6 months Full dissolution within 1–2 years
Biocompatibility	Non-toxic, no inflammatory tissue response No harmful release and/or residence of particles
Mechanical properties	Tensile yield stress TYS>200 MPa, ultimate tensile strength UTS>300 MPa, tensile elongation >15–18% Elastic recoil <4% (in conjunction with stent design)

Stents usually are manufactured in a series of extrusion, drawing, (laser) cutting and (electro-chemical) polishing operations. For magnesium alloy stent tube, the strategy is to realize a possibly fine microstructure, driven by the next considerations.

- Small grains enhance yield stress according to the Hall-Petch relationship with a sensitivity which is typically greater for metals like magnesium that yield by mechanical twinning rather than by dislocation glide [10]. Also, grain refinement reduces (tension-compression) yield anisotropy to become marginal for grains in the micrometer range [11].
- Literature consistently suggests that as grain size decreases, the corrosion resistance of magnesium alloys is improved in neutral and alkaline electrolytes [12], such as blood.
- A coarse microstructure will induce inhomogeneous mechanical and other behavior across the thin walls and struts of the stent as well as add to the risk of large-particle release and/or residence.

From the perspective of process design, it is thus important to understand how the processing parameters affect the microstructural development along the manufacturing chain.

The paper at hand addresses some of the main processing aspects of magnesium alloy stent tube. More in particular, it is concerned with the extrusion and drawing operations. In a further elaboration, equal channel angular pressing is added as a means to refine the microstructure prior to extrusion.

Processing Outline and Adopted Approach

Prior reported efforts on manufacturing magnesium alloy stent tube are based on the route known from conventional metal stents. This consists of (1) hot working of cast feedstock to obtain a solid rod, (2) deep drilling of a hole in the rod to obtain a tube, and (3) multiple cold drawing and intermediate annealing of the tube to reduce diameter and wall thickness [3]. The mesh is subsequently made by laser cutting and the cutting edges are smoothened by electro-chemical polishing. An alternative route departs from this in that the hot working process is conducted by extrusion with a mandrel and tubular billets (enabling the direct manufacturing of seamless tube), and that the drawing is done at elevated temperature (reducing the number of drawing steps) [6].

The processes for manufacturing stent tube that were adopted in the current investigations can be amplified as follows.

Extrusion

In hot extrusion, heated material is pushed through a die, thereby reducing its cross-section to obtain solid or hollow profiles. Although the shape alterations that can be imposed in a single processing step are high, the geometrical tolerances of the obtained extrusions are limited and not high enough to reach the required accuracy of a finished stent tube. Thus hot extrusion is used to provide an intermediary shape. Extrusion is known to impose heavy plastic deformation within the warm-working regime and as such induces dynamic recrystallization and other microstructural effects to the material (e.g., [13]).

The extrusion trials have been conducted using a laboratory extrusion press (make Loire/ACB, 50 t capacity, 1-inch container). In this case the direct extrusion process is conducted with a porthole die, enabling the manufacturing of tube using solid billets. An earlier study has shown that the longitudinal weld seams that are implied by using this kind of tooling are uncritical in terms of ductility for alloys that do readily recrystallize during warm working [14]. Billet size is Ø25×100 mm; tube size is Ø9.5×2 mm, implicating an extrusion ratio (or area-reduction ratio) of R_E=10.4. Billet temperature and extrusion exit speed can be varied between extrusions.

Drawing

In drawing, bar or tube is pulled through a tapered die, thereby reducing the cross-section to obtain a product with the same basic shape. When conducted at room temperature (cold drawing), dimensional accuracy of the product is high, noting that a tolerance in concentricity of the initial tube of for instance ±10% propagates equally into the finished tube. The deformation that can be imposed in a single drawing step is limited so that a substantial reduction in tube diameter and wall thickness can only be achieved by repetitive drawing with progressively smaller tooling. Thus it is used to provide the final shape of the stent tube. Cold drawing is known to induce distortion of the grains and strain hardening of the material. Intermediary heat treatment (annealing) restores ductility but may also provoke microstructural effects like recrystallization and grain growth.

The drawing trials have been conducted by an industrial manufacturer. The implemented variant uses a cylindrical mandrel which passes through the die along with the tube for control of the bore dimension (so-called "moving-mandrel drawing"). In a sequence of drawing steps, the extruded tubes are reduced to Ø1.6×0.13 mm, which is an appropriate geometry for any following *in vivo* (animal) trials to test functionality including bio-compatibility and resorption behavior. Total drawing ratio (or area-reduction ratio) for this sequence is R_D=78.

Equal Channel Angular Pressing

In equal channel angular pressing (ECAP), heated material is repeatedly pushed through an angular die without altering the cross-section to obtain a product with basically the same shape and size. Due to the severe plastic deformation, microstructures can be refined which has been demonstrated to impart favorable

mechanical properties to a variety of materials including magnesium alloys (e.g., [15]). Against this background, it is considered here as a sidetrack of development to potentially improve the quality of the feedstock prior to extrusion.

The ECAP trials have been conducted using the laboratory press that was also used for hot extrusion. In this case a die is installed which redirects the material flow from the container in lateral direction (90° intersection angle). Channel size is Ø25 mm.

Materials and Testing

For the investigations, aluminum-based magnesium alloys were used according to the specifications given in **Table II.** AZ80 is a commercial-grade baseline alloy, while AZM and AZNd are two experimental alloys that include manganese and neodymium as modifiers, respectively. These modifiers are added with the purpose of improving biodegradation properties (notably pitting corrosion resistance) as well as mechanical performance, which was experimentally confirmed [8]. The latter is suggested to be associated with the formation of the Al_8Mn_5 phase in AZM and the $Al_{11}Nd_3$ phase in AZNd. In view of the composition limits for AZ80 (7.8–9.2 wt% Al, 0.20–0.80 wt% Zn, 0.12–0.50 wt% Mn [16]), the baseline alloy turned out to be overdosed with manganese. Apart from the listed elements, traces of copper, iron and nickel (that notably affect corrosion behavior) remain below the common high-purity limits at the parts-per-million level.

Table II. Chemical compositions of the employed AZ alloys (in wt %) – spectrometric analysis.

ALLOY	Al	Zn	Mn	Nd	Mg
AZ80	7.8	0.44	0.93		bal.
AZM	8.1	0.53	0.45		bal.
AZNd	8.0	0.53	0.24	0.55	bal.

AZ80 was available from a commercial supplier in extruded and tempered (T5) condition, while AZM and AZNd were cast as ingots of about 7 kg each in a laboratory setting.

Analysis of the materials during the sequential processing stages was primarily done by means of light optical microscopy (LOM). Microstructures were further characterized with (linear intercept) grain-size measurements. By repeated measurements, including various directions, sections and samples, overall reproducibility is expressed in terms of the standard deviation (typically 10–15 % of the average value) which will be used further on to represent the variation in results.

Results and Discussion

To visualize the intermediate stages in the manufacturing of magnesium alloy stent tube, **Figure 2** shows some cut-out samples of the feedstock/billet, extruded tube, extruded and drawn tube, and finished stent (from left to right).

From the previous section it follows that the quality of the stent tube in terms of its geometrical tolerances, mechanical and corrosion properties will depend (through its microstructure) on the sequence of forming operations and their interaction. Two illustrations of these (inter)relations will be outlined below. The first relates to the working order of hot extrusion followed by cold drawing, the second to ECAP followed by hot extrusion.

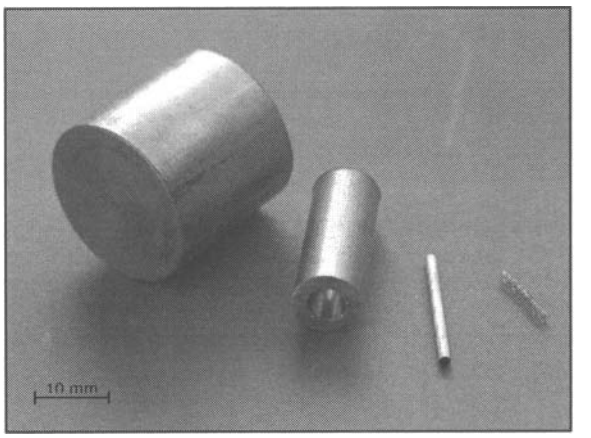

Figure 2. Magnesium alloy stent: from feedstock to finished product.

Extrusion followed by Drawing

Main process parameters during hot extrusion are the degree of deformation (represented by extrusion ratio and die design), the temperature (which in turn depends on starting or billet temperature, degree of deformation and ram speed) and the rate at which the material cools down after processing.

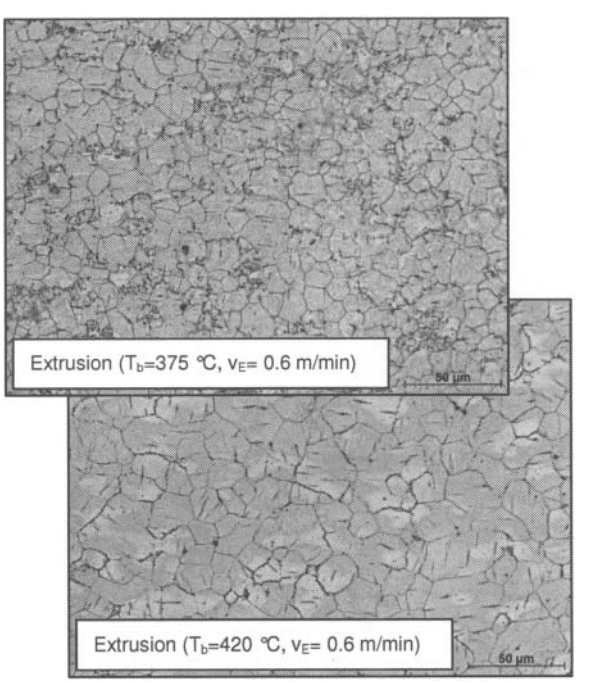

Figure 3. Longitudinal micrographs of AZ80 extruded tube (Ø9.5×2.0 mm) for different billet temperatures.

Figure 3 demonstrates the influence of the billet temperature T_b on the microstructure of the obtained tube for the alloy AZ80. Samples were taken from the last part (the so-called tail) of the extrusion. Extrusion exit speed v_E was kept low in order to avoid hot shortness (surface cracking of the extrusion); further, the tubes were cooled by forced air upon leaving the die. The LOM images

reveal equi-axed, recrystallized microstructures with average grain sizes of 10.7±0.7 µm and 15.2±1.8 µm for the extrusion at T_b=375 °C and T_b=420 °C, respectively. This follows the general notion that extrusion temperature should be kept as low as possibly permitted by the press capacity to reach a fine microstructure (e.g., [17]).

Figure 4 shows microstructures of extruded tubes for the three alloys, again by taking samples from the tail of the extrusion. Extrusion settings were identical, including the forced air cooling. The LOM images reveal equi-axed, recrystallized microstructures. For AZ80, precipitates show at the grain boundaries, while for AZM and AZNd (fragmented) intermetallic compounds appear rather as stringers oriented in the extrusion direction. Average grain size is typically in the 10 µm range, but it should be noted that AZ80 on the one and AZM and AZNd on the other hand cannot be directly compared as the former started from a pre-extruded billet (average grain size ~13 µm) and the latter from as-cast billets (200–300 µm).

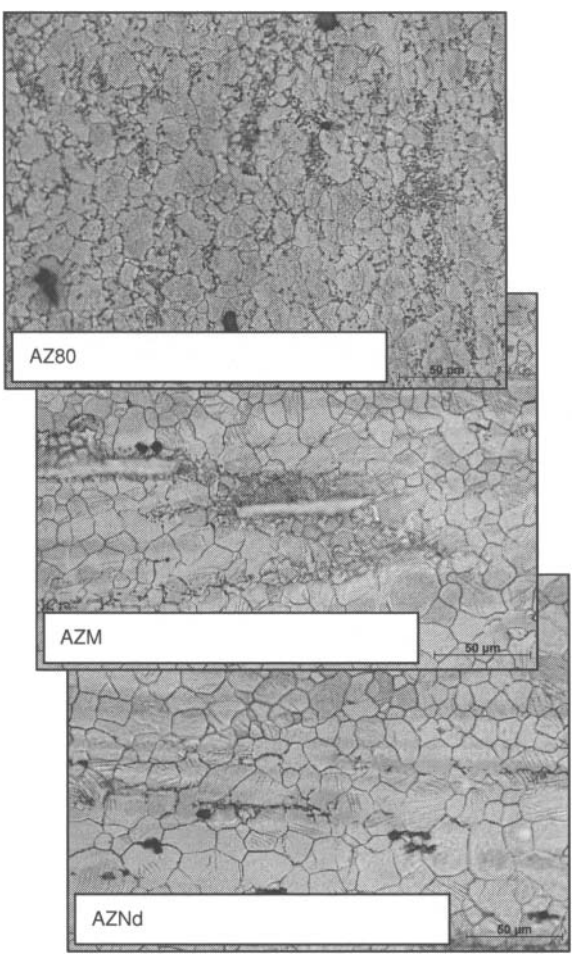

Figure 4. Longitudinal micrographs of extruded tube (∅9.5×2.0 mm; T_b=375 °C, v_E=0.3 m/min).

Main process parameters during cold drawing are the degree of deformation (represented by drawing ratio and die designs), the drawing and annealing sequence (partitioning into individual drawing and annealing steps), and the annealing parameters (temperature and time).

Figure 5 shows microstructures of finished drawn tubes for the three alloys (starting with extruded tubes as depicted in Figure 4). Intermediate annealing temperature followed an initial recommendation of 385 °C for AZ80 [16], but was fine-tuned somewhat in conjunction with the drawing operations. Further a heat treatment was carried out at 340 °C after the final drawing step. The LOM images reveal equi-axed, re-crystallized microstructures with average grain sizes typically in the 30 µm range. Similar microstructures appear after each intermediate annealing step, supporting the view that static recrystallization is the underlying mechanism.

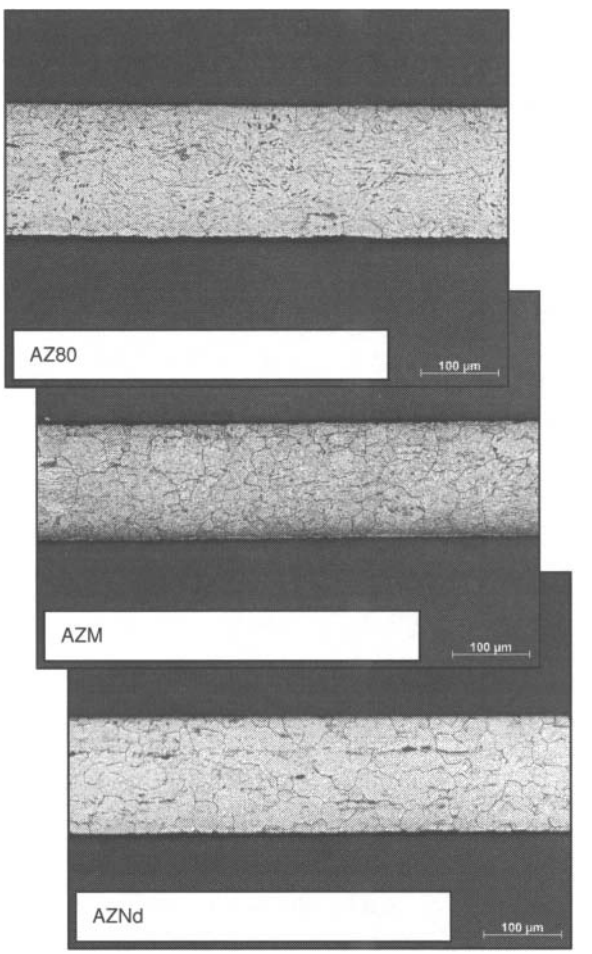

Figure 5. Longitudinal micrographs of extruded and drawn tube (∅1.6×0.13 mm).

Figure 6 summarizes the development of the average grain size for the three alloys during the successive manufacturing steps. Extrusion refines the microstructure for all alloys to a similar extent. Notably, an earlier investigation with these alloys in which ∅5 mm bars were extruded with the same set-up and under comparable conditions yielded finer as-extruded microstructures (average grain size typically 5 µm) [8]. Extrusion of hollow sections through a porthole die generally requires more

mechanical work than extrusion of solid sections and as a consequence entails more generated heat and associated higher temperatures, so that grain growth is likely to have a larger effect in these cases. Further, subsequent drawing at room temperature (RT) with intermediate heat treatment (HT) coarsens the microstructure, where the effect appears to be marginally more pronounced for AZ80 and AZM than for AZNd.

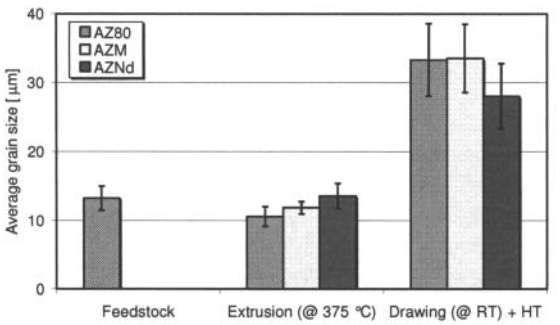

Figure 6. Microstructural evolution during the extrusion-drawing sequence.

Equal Channel Angular Pressing followed by Extrusion

Main process parameters during ECAP are the degree of deformation (represented by die design and number of passes) and the temperature (which in turn depends on starting or billet temperature and ram speed).

Figure 7 shows microstructures for the three subsequent stages of the concerned manufacturing sequence for AZ80. In ECAP the temperature of the billet and chamber were set at T_b=275 °C, with the billets being reheated between the passes. As for billet orientation, samples were reversed and turned 90° between individual passes. ECAP effectively refines the microstructure to an average grain size of about 3 µm after three passes which does not further decrease within the explored range of up to nine passes. After extrusion, however, average grain size has increased to the 10 µm range. Microstructures remain essentially equi-axed at the successive stages, suggesting that dynamic recrystallization is the predominant effect that determines the microstructural evolution.

Figure 8 summarizes the development of the average grain size for the three alloys during the successive manufacturing steps. After ECAPing (which involved nine passes), the average grain size ranges between 3 and 5 µm, with some variation between the alloys. As a result of the following extrusion process, average grain size increases for all alloys to a similar extent and comparable to those obtained without prior ECAPing (already presented in Figure 6).

Table III lists the microstructural results for some series of extrusion trials without and with prior ECAPing. From this it appears that the influence of ECAP on the average grain size of the semi-finished tube is marginal if not insignificant. Within the explored settings, billet temperature in the extrusion process is the most effective parameter for controlling eventual grain size.

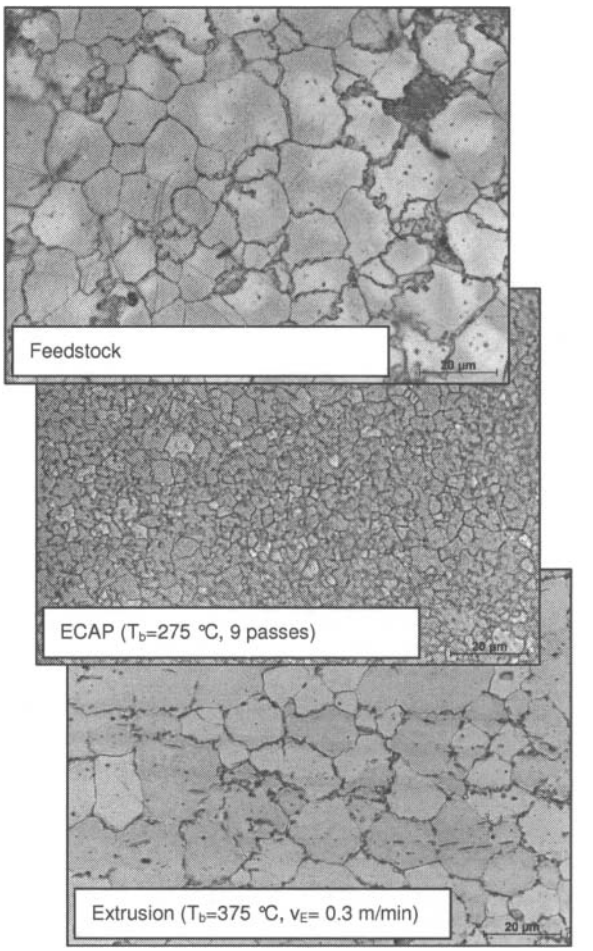

Figure 7. Longitudinal micrographs of AZ80 for successive stages of the ECAP-extrusion sequence.

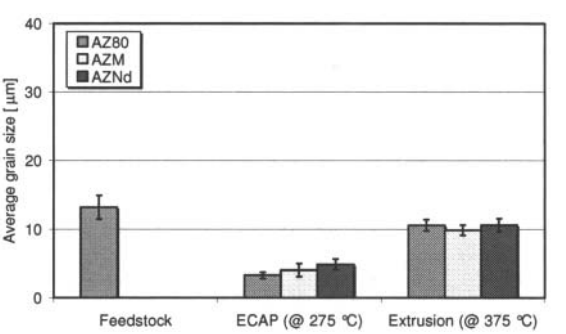

Figure 8. Microstructural evolution during the ECAP-extrusion sequence.

Table III. Average grain size of semi-finished tube (Ø9.5×2.0 mm) in dependence on the processing route.

T_b	ALLOY	EXTRUSION (@ T_b)	ECAP (@ 275 °C) + EXTRUSION (@ T_b)
375 °C	AZ80	10.5±1.4 µm	10.6±1.4 µm
	AZM	11.8±0.9 µm	9.8±1.0 µm
	AZNd	13.5±1.8 µm	10.6±1.3 µm
325 °C	AZ80	6.5±0.4 µm	7.7±0.8 µm
	AZM	7.9±0.7 µm	5.7±0.7 µm
	AZNd	8.3±1.0 µm	5.9±0.9 µm

Conclusions and Outlook

Results of the reported work can be recapitulated as follows.

- Stent tube can be manufactured from the baseline alloy AZ80 as well as from the experimental alloys AZM and AZNd by a sequence of extrusion and drawing operations. The microstructure of the obtained stent tube (average grain size ~30 µm) is still on the coarse side in view of the wall thickness and strut size of the tube mesh (~100–150 µm).
- Hot extrusion refines the microstructure by thermo-mechanically induced dynamic recrystallization, while subsequent cold drawing with intermediate annealing results in grain coarsening due to static recrystallization.
- ECAPing of the material prior to the extrusion-drawing sequence effectively refines the microstructure to an average grain size of 3–5 µm. The fine grains, however, are not maintained during subsequent extrusion, so that its effectiveness to improve feedstock quality is limited.

Based on the previous, possible means to advance the efficiency and quality of the current manufacturing route for magnesium alloy stent tube are to better attune the extrusion and the drawing process (in order to optimize microstructural development versus geometrical accuracy), and to better attune the order of the individual drawing operations in conjunction with intermediate annealing (in order to reduce grain growth during this stage of manufacturing). On a higher level of innovation, cold drawing may be replaced by a combined warm-cold drawing process with the objectives of enhancing microstructural control and simultaneously improving manufacturing efficiency while maintaining geometrical tolerances. On a fundamental level, textural development could be monitored "through process" with such methods as electron back-scatter diffraction in order to enhance the basic understanding of microstructural development versus (directionality of) mechanical properties.

References

1. D. Apelian, "Looking beyond the last 50 years: The future of materials science and engineering", *JOM*, 59 (2) (2007), 65–73.

2. M.P. Staiger, A.M. Pietak, J. Huadmai, G. Dias; "Magnesium and its alloys as orthopedic biomaterials: A review", *Biomaterials*, 27 (2006), 1728–1734.

3. B. Gerold, H. Müller, "Konzept für biologisch abbaubare Implantate aus Magnesium", *4. Ranshofener Leichtmetalltage 2006 – Vom Werkstoff zum Bauteilsystem*, LKR-Verlag, Ranshofen Austria (2006), 173–183.

4. H. Müller, "Biodegradation von Magnesiumlegierungen – Ein neues Konzept für temporäre Gefäßimplantate", *5. Ranshofener Leichtmetalltage 2008 – Zukunft // Leichtmetalle von der Forschung in die Anwendung*, LKR-Verlag, Ranshofen Austria (2008), 111–123.

5. C.Z. Deng, R. Radhakrishnan, S.R. Larsen, D.A. Boismer, J.S. Stinson, A.K. Hotchkiss, E.M. Petersen, J. Weber, T. Scheuermann, "Magnesium alloys for bioabsorbable stents: A feasibility assessment" – *this proceedings volume.*

6. Th. Hassel, F.-W. Bach, A.N. Golovko, "Production and properties of small tubes made from MgCa0,8 for application as stent in biomedical science", *Proceedings of the 7th International Conference on Magnesium Alloys and Their Applications*, Wiley-VCH, Weinheim (2006), 432–437.

7. M. Erinc, W.H. Sillekens, "An assessment on modified AZ80 alloys for prospect biodegradable CV stent applications", *Proceedings of the 8th International Conference on Magnesium Alloys and Their Applications*, Wiley-VCH, Weinheim (2010), 1201–1207.

8. M. Erinc, X. Zhang, W.H. Sillekens, "Modified AZ80 magnesium alloys for biomedical applications", TMS, *Magnesium Technology 2010*, (2010), 641–646.

9. M.A. Leeflang, J. Zhou, J. Duszczyk, "Deformability and extrusion behaviour of magnesium-lithium binary alloys for biomedical applications", *Proceedings of the 8th International Conference on Magnesium Alloys and Their Applications*, Wiley-VCH, Weinheim (2010), 1182–1188.

10. M.R. Barnett, "A rationale for the strong dependence of mechanical twinning on grain size", *Scripta Materialia*, 59 (2008), 696–698.

11. J. Bohlen, P. Dobron, E.M. Garcia, F. Chmelík, P. Lukáč, D. Letzig, K.-U. Kainer, "The effect of grain size on the deformation behaviour of magnesium alloys investigated by the acoustic emission technique", *Advanced Engineering Materials*, 8 (5) (2006), 422–427.

12. K.D. Ralston, N. Birbilis, "Effect of grain size on corrosion: A review", *Corrosion*, 66 (7) (2010), 075005/1–13.

13. S. Müller, K. Müller, W. Reimers, M. Rosumek, "Microstructure development of extruded Mg alloys", TMS, *Magnesium Technology 2005*, (2005), 165–170.

14. W.H. Sillekens, D.C.W. van der Linden, A.J. den Bakker, "Weld-seam quality of hollow magnesium alloy extrusions", TMS, *Magnesium Technology 2008*, (2008), 189–194.

15. Y. Yan, G. Sun, B. Wei, Y. Hu, "Influence of thermoplastic ECAP on mechanical properties and microstructures of an AZ61A magnesium alloy", TMS, *Magnesium Technology 2004*, (2004), 97–100.

16. M.M. Avedesian, H. Baker, eds., *Magnesium and Magnesium Alloys – ASM Specialty Handbook* (Materials Park, OH: ASM International, 1999), 260–261.

17. Y. Uematsu, K. Tokaji, M. Kamakura, K. Uchida, H. Shibata, N. Bekku, "Effect of extrusion conditions on grain refinement and fatigue behaviour in magnesium alloys", *Materials Science and Engineering A*, 434 (2006), 131–140.